Energy return in running surfaces

Document status and date:
Published: 01/01/1994

Document Version:
Publisher's PDF, also known as Version of Record (includes final page, issue and volume numbers)

Please check the document version of this publication:

• A submitted manuscript is the version of the article upon submission and before peer-review. There can be important differences between the submitted version and the official published version of record. People interested in the research are advised to contact the author for the final version of the publication, or visit the DOI to the publisher's website.
• The final author version and the galley proof are versions of the publication after peer review.
• The final published version features the final layout of the paper including the volume, issue and page numbers.

[Link to publication](#)

Energy Return in Running Surfaces

B. J. E. van Rens
WFW-rapport 94.151

Abstract

Running surfaces are estimated to account for up to one percent of the energy necessary for running. How much of this energy is dissipated in the surface and how much is returned to the runner is not known. A method has been designed to calculate the energy that is absorbed and returned by a running surface. In this method the time of energy return is of importance. Energy can only be returned if this return coïncides with the take off phase. A two dimensional finite element model (FEM) was generated to calculate the energy. Linear elastic, plane strain elements with linear Rayleigh damping were used. Data obtained by a force platform for toe running were used as input for the model. The FEM consisted of two layers of surface of which the stiffness was varied independently. Additionally, the Rayleigh damping ratio for the whole model was varied. The results indicate that there are combinations of top layer stiffness, bottom layer stiffness and damping ratio for which the performance of the surface from an energy standpoint is optimal. The results indicate that very stiff surfaces do not necessarily improve performance.

Contents

Chapter 1

Introduction

The performance of a runner depends, among other aspects, on the amount of energy available in the athlete's body, the speed at which this energy can be released, and the amount of energy needed by the runner to run a certain distance. The focus in this report will be on the reduction of the amount of energy needed for a certain achievement.

The amount of energy used for running a race depends, among other factors, on the energy absorbed by the body and the energy absorbed by elements other than the body. These other elements include drag, shoes and running surface. Drag is a factor which is difficult to change in running. The shoes are estimated to account for about 3 percent of the energy dissipated in running [12]. Research also indicates that the stiffer the sole of the running shoe the less energy will be dissipated in the sole [8]. Frederick at al., however, showed that the amount of energy dissipated in running does not follow the trend of the energy dissipated in the sole [5]. Lately, an interest has developed for the third factor, the running surface, since there is evidence that certain surfaces can induce overuse injuries [6, 11]. Research also indicates that the stiffness properties of a surface can influence running performance [9] and can influence jumping heights of volleyball players [17]. Running surfaces are estimated to absorb one percent of the energy of locomotion [12].

The purpose of this project, therefore, was to discuss the return of energy from a running surface for toe running for a surface built of two layers. Since the body can only use external energy at specific moments the energy produced by the track is only considered returned energy if the moment of energy production coincides with a moment at which the body can use this

energy for take-off.

The goal of this project is achieved by first applying the first law of thermodynamics to toe running. The mechanisms involved in absorption and returning of energy are dealt with on a mechanical one-dimensional level in Chapter 2. This renders an algorithm to calculate the energy used in toe running. A Finite Element Model, necessary to calculate the displacements of the surface, is presented in Chapter 3. The mesh and the boundary conditions are presented together with the material properties used to approximate the running surface. The results are presented in Chapter 4. These results are discussed in Chapter 5. The results are explained and tested for validity. Finally, the conclusions are drawn in Chapter 6.

Chapter 2

The Energy-Equation in Running

2.1 Energy equation

The first law of Thermodynamics states that for any body that interacts with its surroundings Equation 2.1 applies,

$$dQ + dW = dU \qquad (2.1)$$

where:
dQ = the change in thermal energy stored in the body
dW = the change in external energy exerted on the body
dU = the change in internal energy of the body

Since dQ represents the changes in thermal energy or chemical consistency of the body and this report deals with running surfaces which can be assumed adiabatic this term is assumed to be zero and can be neglected. This renders Equation 2.2.

$$dW = dU \text{ or, } W = U + Constant \qquad (2.2)$$

In other words: The energy put into a body externally, for instance by exerting a force on it and displacing it concurrently, equals the internally stored energy, for instance the elastic energy of the body.

2.2 External energy, W

The external energy put into a body by a force acting upon a point of that body is calculated by multiplying the force by the distance the point has travelled. If the force is not constant over the trajectory that the body follows but depends on the position of the body, the velocity of the body and/or the time then the external energy exerted on the body can be calculated as shown in Equation 2.3.

$$W_{a-b} = \int_{\vec{x}_a}^{\vec{x}_b} \vec{F}(\vec{x}, \dot{\vec{x}}, t) \cdot \vec{ds} \qquad (2.3)$$

where:

W_{a-b} = the external energy put in by the force moving the point on the body between a and b

$\vec{F}(\vec{x}, \dot{\vec{x}}, t)$ = the force as a function of the position $\vec{x}$, the velocity $\dot{\vec{x}}$, and the time t

$\vec{ds}$ = the place differential along the path that the point follows

In the case of calculations within discrete time steps the change in external energy can be calculated as shown in Equation 2.4.

$$W_{a-b} = \sum_{i=2}^{n} \vec{F}_i \cdot (\vec{x}_i - \vec{x}_{i-1}) \qquad (2.4)$$

where:

$\vec{F}_i$ = the force at time t_i

$\vec{x}_i$ = the position at time $t - i$

t_1 = the time of touch-down

t_n = the time of toe-off

The forces acting on the surface can be approximated by using data from a force plate with a surface mounted on top of the forceplate. Research indicates that changing the properties of running surfaces has little effect on the magnitude of forces for the shoe-surface interface [13]. This is, among other factors, due to the fact that the runner adjusts to varying surface conditions to keep the impact forces on the body at the same level [4].

The displacements, $x_i - x_{i-1}$, are obtained by calculating the displacements of the surface under a certain force. Section 2.3.1 will deal with the displacements in more detail.

2.3 Internal energy, U

The terms energy absorption and energy return have to be defined before these terms can be applied to discuss energy-equations in running. For the sake of simplicity, a one-dimensional situation will now be considered. However, the principles that will be discussed can be transferred into three-dimensional applications.

A spring absorbs energy when the direction of the deformation and the direction of the force working on the spring are the same. It returns energy when the direction of deformation and the direction of force are opposite. In other words: A body returns energy when the change in internal energy, dU, in Equation 2.2 is negative and it absorbs energy when the change in internal energy is positive.

In accordance with Equation 2.4 for the change in external energy, W_{a-b}, we can split the change in internal energy, U_{a-b}, into a summation over discrete time intervals. This renders Equation 2.5.

$$U_{a-b} = \sum_{i=2}^{n} (U_i - U_{i-1}) \tag{2.5}$$

where:
U_{a-b} = the change in internal energy between points a and b
$U_i - U_{i-1}$ = the change in internal energy over the time interval i

Splitting the Equation 2.5 for discrete time-intervals into an equation for the absorbed internal energy U_{abs} and an equation for the returned energy U_{ret} renders Equations 2.6. The (a-b)-subscript will be ommitted from now on.

$$U_{tot} = U_{abs} - U_{ret} \tag{2.6}$$

where U_{abs} and U_{ret} can be calculated with the following algorithm:

```
U_abs=0;U_ret=0;
for i=2 to n
    if (U[i] - U[i-1]) > 0
        U_abs = U_abs + (U[i] - U[i-1])
    else
        U_ret = U_ret - (U[i] - U[i-1])
    end if
end for
```

By putting the equations for U_{abs} and U_{ret} into Equation 2.6, Equation 2.5 is formed again. This notation, however, gives an indication of how much energy is put into the surface and how much is returned rather than an overall value of the total loss of energy into the system. In the following sections the U_{abs} and the U_{ret} will be discussed in more detail. Again, for the sake of simplicity only the one dimensional situation will be discussed.

2.3.1 Absorbed internal energy, U_{abs}

The energy put into the surface is mainly stored in the form of elastic energy. A small part will be stored in the form of kinetic energy of the surface and/or potential energy. Equation 2.7 gives the formula for the total absorbed energy. In this equation k_r is a function of the position s and the speed $\dot{s}$ of the point on the surface upon which the force acts. This renders:

$$U_{abs} = \int_{x_0}^{x_{max}} k_r(s, \dot{s})s.ds + U_{kin} + U_{height} \qquad (2.7)$$

with

$$k_r(s, \dot{s}) = \frac{1}{s} \cdot F_{int}(s, \dot{s}) \qquad (2.8)$$

where:

U_{abs} = the absorbed energy between impact and maximum deflection of the surface

F_{int} = the internal forces, working from within the surface

k_r = the stiffness of running surface

U_{kin} = the kinetic energy.

U_{height} = the energy from elevating the center of gravity

x_0 = the position of the surface at impact of the shoe

x_{max} = the position of the surface at the maximum deflection of the surface

s = the integration variable that follows the deformation history

In reality the surface elastomeres are nonlinear visco-elastic which means that the stiffness of the surface is given by Equation 2.9 [15].

$$k_r = k_{static}(s) + \frac{b\|\dot{s}\|}{s} \tag{2.9}$$

where

k_{static} = the time dependent stiffness of the rubber surface as a function of displacement

b = the viscous coëfficient of the rubber surface

Entering Equation 2.9 into Equation 2.7 and simplifying it renders Equation 2.10.

$$U_{abs} = \int_{x_0}^{x_{max}} (\frac{b\|\dot{s}\|}{s} + k_{static}(s))s.ds + U_{kin} + U_{height} \tag{2.10}$$

This equation states that of all the internal energy (which in this case is equal to the external energy as is shown in Section 2.1) is directed towards kinetic, height, and viscous energy. The absorbed energy still remaining after these three causes the displacement of the surface. Equation 2.10 holds true for one dimensional situations with the surface consisting of one component. However if more components were used and the problem is broadened to a 3-dimensional situation Equation 2.10 would not hold true. The complexity of the problem would make it virtually impossible to solve it analytically and therefore one would have to resort to solving Equation 2.7 numerically.

2.3.2   Returned internal energy, U_{ret}

Three of the four components that constitute Equation 2.10 are stored energy that can be retrieved from the system. The viscous component of the rubber absorbs energy in such a way that it can not be retrieved. The energy that can be retrieved from a rubber surface is given by Equation 2.11

$$U_{ret} = \int_{x_{max}}^{x_{to}} (-\frac{b\|\dot{s}\|}{s} + k_{static}(s))s.ds + U_{kin} + U_{height} \qquad (2.11)$$

where:

x_{max} = the position of the surface at maximum deflection

x_{to} = the position of the surface at toe off

The returned energy equals the stored energy minus the viscous energy dissipated by the surface moving back to its original position. The path the surface follows to its original position is most likely not the same as the path followed during the initial deformation. Therefore, the viscous component of Equation 2.11 will not be of the same magnitude as the viscous component in Equation 2.10.

Equations 2.10 and 2.11 could give the impression that by making the viscous coefficient of rubber zero all the energy put into the surface will also be returned. This is not the case. During a stride, the stance leg uses energy to absorb the heel impact and to generate a toe push-off. The energy that the body loses upon landing is partly stored in the surface and partly in the sole of the shoe. The body is not able to store a significant amount of energy in its elastic components [10]. This means that all the energy returned to the runner during heel impact will not be stored anywhere in the leg and, consequently, is lost. More over, this energy will have to be absorbed by the leg and this costs as much energy as the amount of energy to be absorbed. This means that the internal energy of the surface has to be returned during the take-off phase to contribute to the energy of locomotion. The take-off phase is defined as the second half of the time period of the stance phase. Therefore all the energy returned in the second half of the stance phase contributes to U_{ret}. Considering this "time- dependence" of the energy return we adjust the algorithm found in Section 2.3 to read:

```
U_abs=0;U_ret=0;
for i=2 to n
    if (U[i] - U[i-1]) > 0
        U_abs = U_abs + (U[i] - U[i-1])
    else
        if (i¡i_take-off-phase)          i_take-off-phase is the interval when
            U_abs = U_abs - (U[i] - U[i-1])              the take-off phase starts
        else
            U_ret = U_ret - (U[i] - U[i-1])
        end if
    end if
end for
```

2.4   Energy Return Ratio

To assess the performance of a surface in view of returning energy at the right time, a value has to be given to each surface. The focus of this report lies on the energy equations in the anterior- posterior (a-p) direction and the proximal-distal (p-d) direction. For each direction the external forces are known through force plate data and thus the internal energy can be calculated. In each direction this renders an amount of energy that is absorbed by the surface, $U_{abs}{}^{a-p}$ and $U_{abs}{}^{p-d}$, and an amount of energy returned by the surface, $U_{ret}{}^{a-p}$ and $U_{ret}{}^{p-d}$. To calculate the performance of a surface the Energy Return Ratio, ERR, is used. The ERR consists of an a-p component and a p-d component.

$$ERR = \alpha_1 ERR_{a-p} + \alpha_2 ERR_{p-d} \quad \text{with} \quad \alpha_1 + \alpha_2 = 1 \qquad (2.12)$$

with

$$ERR_{a-p} = \frac{U_{ret}^{a-p}}{U_{abs}^{a-p}} \quad \text{and} \quad ERR_{p-d} = \frac{U_{ret}^{p-d}}{U_{abs}^{p-d}} \qquad (2.13)$$

where:

α_1 and α_2 = weight factors that indicate the weight of the ratios for each direction. These factors can be chosen to accommodate different sports.

ERR_{a-p} = the Energy Return Ratio in a-p direction

ERR_{p-d} = the Energy Return Ratio in p-d direction

U_{ret}^{a-p} = the returned energy in a-p direction

U_{abs}^{a-p} = the absorbed energy in a-p direction

U_{ret}^{p-d} = the returned energy in p-d direction

U_{abs}^{p-d} = the absorbed energy in p-d direction

2.5 Dissipated Energy

Another indicator of the performance of a running surface is the amount of dissipated energy. The dissipated energy is calculated as described by Equation 2.14 and is the energy that remains in the surface after take-off. The energy that is dissipated in a surface is energy that a runner has to generate in addition to the energy of locomotion. For that reason the amount of dissipated energy should be as low as possible.

$$U_{dis} = U_{abs} - U_{ret} \qquad (2.14)$$

where:

U_{dis} = the amount of energy that is dissipated in the surface

Combining Equation 2.14 and Equation 2.13 renders Equation 2.15.

$$U_{dis} = U_{abs}(1 - ERR) \qquad (2.15)$$

Equation 2.15 reveals that a low amount of dissipated energy can be achieved by having a high energy return ratio or by keeping the absorbed energy low.

The introduction of the U_{dis} renders the following dilemma. Consider two surfaces. Surface 1 has an ERR of 0.8 and an U_{abs} of 5 Joules. Surface 2 has an ERR of 0.8 and an U_{abs} of .5 Joule. This means that surface 1 has a U_{dis} of 1 Joule and a U_{ret} of 4 Joules. Surface 2 has an U_{dis} of 0.1 Joules and a U_{ret} of 0.4 Joules. In other words surface 1 is more favourable in terms of U_{ret} but surface 2 is more favourable considering the U_{dis}. At this moment it is not clear which of these surfaces should be chosen. Or in more general terms it is not clear wether it is more important to have a low U_{dis} or a high U_{ret}. However, it should be noted that the U_{ret} is a measure of how much energy is being returned at the moment of take-off and $U_{ret} = ERR \cdot U_{abs}$. A high value for U_{ret} is obtained with a high U_{abs} but a low U_{dis} is reached by keeping U_{abs} low. U_{ret} is a measure of how much higher the take-off speed is compared to the situation where no energy is returned. A higher take-off speed implies longer strides which means that fewer strides are needed to run a distance. Therefore, a high U_{ret} (and therefore a higher U_{abs}, Equation 2.13) can be more important than a low U_{dis} as long as the positive effects of the higher U_{ret} outweigh the higher U_{dis}. In other words, it is acceptable to store a certain amount of energy in the surface as long as most of this energy is returned at the right time to help in take- off.

In summary, a surface should be optimized for a high value of the ERR while caution is taken to ensure that the U_{abs} remains within an acceptable value. The size of that value can only be assessed if the human body is included in the model or if testing is done with runners on running surfaces with different combinations of ERR and U_{abs} to compare the performance of the runners across the surfaces.

Chapter 3

Finite Element Model

This Chapter discusses the mesh that is used and the way the material is modelled. The model of the surface was generated with the finite element pre-processor of PATRAN, a finite element program. The mesh obtained in PATRAN was exported to the general purpose non-linear finite element program ABAQUS. In ABAQUS complex boundary conditions and the material properties of the surface were added. Then the calculations were done in ABAQUS using its nonlinear dynamic module. The results of these calculations were post-processed with software written in MatLab using the algorithm introduced in Chapter 2.

3.1 Finite Element Mesh

The surface was modelled as a two dimensional cross cut, using plane strain elements. The x- axis direction represented the anterior-posterior direction and the y-axis direction the proximal- distal direction(See also Figure 3.1). The surface was split in two layers that each had a range of material properties. The top layer had a thickness of 7.0 mm and the bottom layer a thickness of 10.0 mm. This is comparable to the surfaces currently used for runningtracks [15]. By changing the characteristics of each layer the effect of combinations of material properties on energy return could be studied. The contact area of the foot for toe running was considered to be 50.0 mm by 50.0 mm. The total length of the modelled surface was 100.0 mm (See also Figure 3.2).
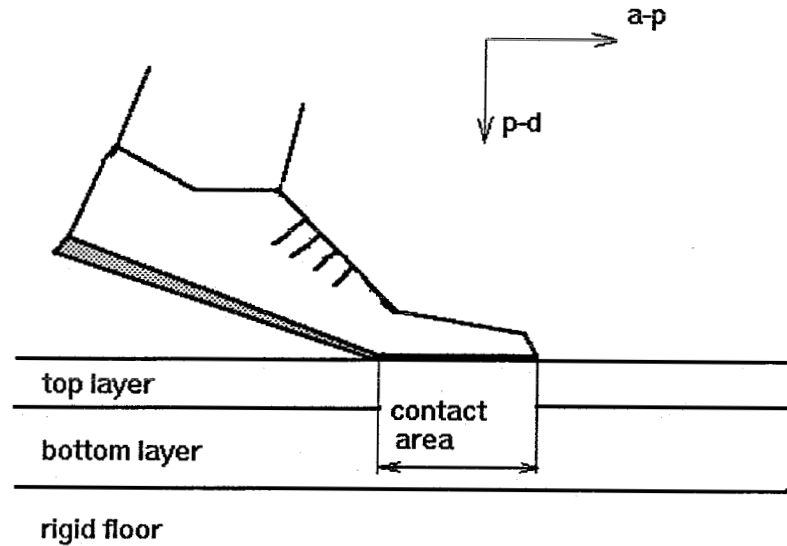
Figure 3.1: Schematic representation of the two-layer surface with the running shoe. The directions are indicated.

The mesh was generated by using twenty elements horizontally and three vertically for the top layer and four elements for the bottom layer. The elements used were two dimensional quadratic elements with eight nodes. The elements had unit thickness in the third direction, and the degrees of freedom were only the displacements in the plane of analysis.

The nodes at the bottom of the surface were fully constrained to account for these nodes being glued to the underlying, rigid surface. The nodes at the sides of the surface were constrained in horizontal or anterior-posterior direction to account for the surface that was not modelled. The surface that is not modelled would normally resist against being pushed away in horizontal direction. The length of the nonloaded surface, five elements on each side, was sufficient to ensure no edge effects would occur. The strains at the boundaries of the model remained below 3 percent of the values directly under the contact area.
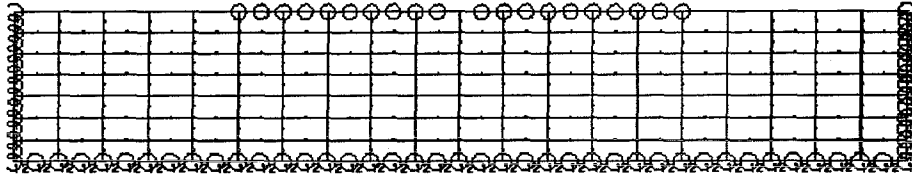
Figure 3.2: Schematic representation of the mesh for the 2-D surface with boundary conditions and MPC.

The contact area was considered rigid, which means that the nodes in the contact area always remained on a straight line. This was done by using a Multi Point Constraint (MPC) in ABAQUS. The contact area was considered rigid to account for the use of spike-shoes on running tracks. These spike-shoes have a rigid plate under the forefoot to enable the metal spikes to be screwed into the shoe. Also, a rigid deformation area facilitates the calculation of the energy that is absorbed and returned. The impact force was distributed evenly across the 10 elements of the contact area. Since the thickness of the elements is 1 mm instead of 50 mm the force applied to the slice of surface that was modelled could be calculated through Equation 3.1.

$$F_{lin} = F_{tot}/50 \qquad (3.1)$$

where:
F_{lin} = the force acting on the slice of surface that is modelled
F_{tot} = the force acting on the total surface

The force had to be applied to the nodes of the elements. The 10 elements that constituted the contact area had 21 nodes. The force on each node in center of the contact area could be calculated with Equation 3.2.

$$F_{nod} = F_{lin}/20 \qquad (3.2)$$

where:
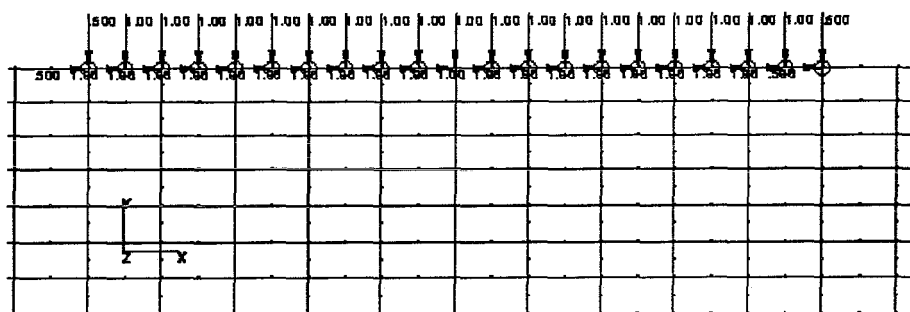F_{nod} = the force that worked on one node of the surface

Figure 3.3: The distribution of the load on the nodes of the contact area. The two nodes at the edge are loaded with half the load of the other nodes.

The two nodes on the edge of the contact area were different to the rest. The two nodes on the edge only had pressure on one element they are connected to, as opposed to the other nodes that had pressure on both elements they were connected to. This means that these two outside nodes were loaded with half of the force calculated in Equation 3.2. It can easily be seen that with $21 - 2 = 19$ nodes loaded with F_{nod} and two nodes loaded with half F_{nod} left $20 * F_{nod}$, which equaled F_{lin}. The distribution of the forces can be seen in Figure 3.3. This way of modelling would introduce an error since the model uses quadratic elements. To model pressure on quadratic elements the forces on the nodes of the element should not be equal. The force should have a ratio of 1 to 4 to 1 for the edge node, the center node and the other edge node of an element. This would render a pattern of 1:4:2:4:....:4:2:4:1 instead of the 1:2:2:....:2:2:1 that was modelled now. However, the used method introduces no errors since a MPC is used which distributes the forces correctly across the nodes. The advantage of the used method is that it facilitates the modelling.
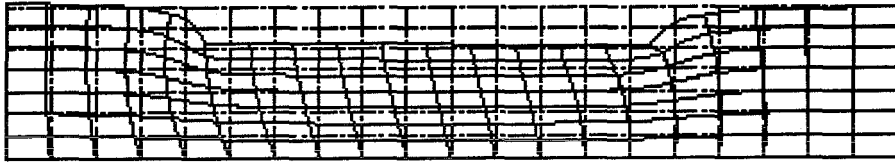
Figure 3.4: The undeformed mesh (dotted) and the deformed mesh (lines). The mesh was deformed with both a-p and p-d loading.

In Figure 3.4 the effect of the MPC can be seen for a loaded situation.

3.2 Material Properties

Running surfaces consist of a vulcanised rubber that has granules mixed into it. Rubber can be considered an incompressible polymer since the volume change under compression is relatively small [1]. Rubber can undergo tensile strains greater than 100 percent without breaking. The stress-strain relationship for compression is not linear (Figure 3.5) which implies that rubber should be modelled as a nonlinear elastic material. ABAQUS has the possibility to model the rubber properties with "Hyperelastic"-elements. These are elements with a nonlinear stress-strain relationship. The stress-strain relationship is approximated by a polynomial function in which the parameters have to be calculated from test data.

Rubberlike polymers display a speed-dependent viscoelastic behaviour [7] which causes damping of vibrations. The damping that is used in ABAQUS is "Rayleigh"- damping which is proportional to the elasticity of the material. This damping adds a stress component to the stress-strain relationship that describes the surface. This stress component can be calculated with Equation 3.3.
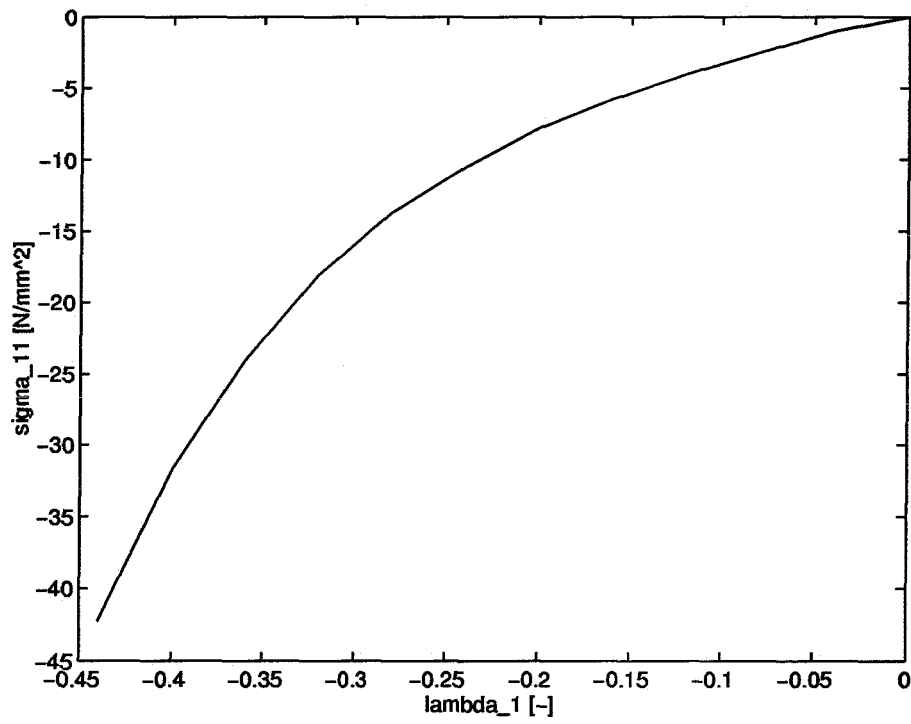
Figure 3.5: The stress-strain curve for one of the samples of rubber which was compressed with a speed of 1 mm/min until $\lambda_1 = -0.44$ (λ_1 is the uniaxial strain defined as $\Delta l/l$).

$$\sigma^D = \beta_R D^{el} : \dot{\varepsilon} \qquad (3.3)$$

where:
σ^D = the tensor representing the additionally generated stress
β_R = the Rayleigh damping coefficient
D^{el} = the elasticity tensor of the material
$\dot{\varepsilon}$ = the strain rate

ABAQUS needs the elasticity tensor of the material which is generated in the module "Elastic" to imply Equation 3.3 for damping. The Elastic and the Hyperelastic module are mutually exclusive. This means that the use of Hyperelastic elements and Rayleigh damping in the same model is not possible. Since the damping of rubber is an important property and needs to be included, the elastic properties of rubber were approximated with a linear elastic element. Figure 3.6 displays the normalized stress versus the normalized strain for one of the samples of the surface and for the linear approximation of that surface. Since the stresses remain below 1.5 N/mm^2 the linear approximation does not introduce a significant error.

Rubber also displays a time-dependent visco-elastic behavior that can be described by Mooney- Rivlin ([3]) or by the Prony series ([16]). In this project the Prony series were used. Equation 3.4 displays the Prony series representation for stress relaxation. This equation gives the relation between the time-dependent shear modulus and the instantaneous shear modulus as a function of time.

$$G_R(t) = G_0(1 - \sum_{i=1}^{N} \bar{g}_i^P (1 - e^{-t/\tau_i})) \qquad (3.4)$$

where:
$G_R(t)$ = the time-dependent shear modulus
G_0 = the instantaneous shear modulus
$\bar{g}_i^P$ = the Prony series shear relaxation modulus
t = the time since the application of force
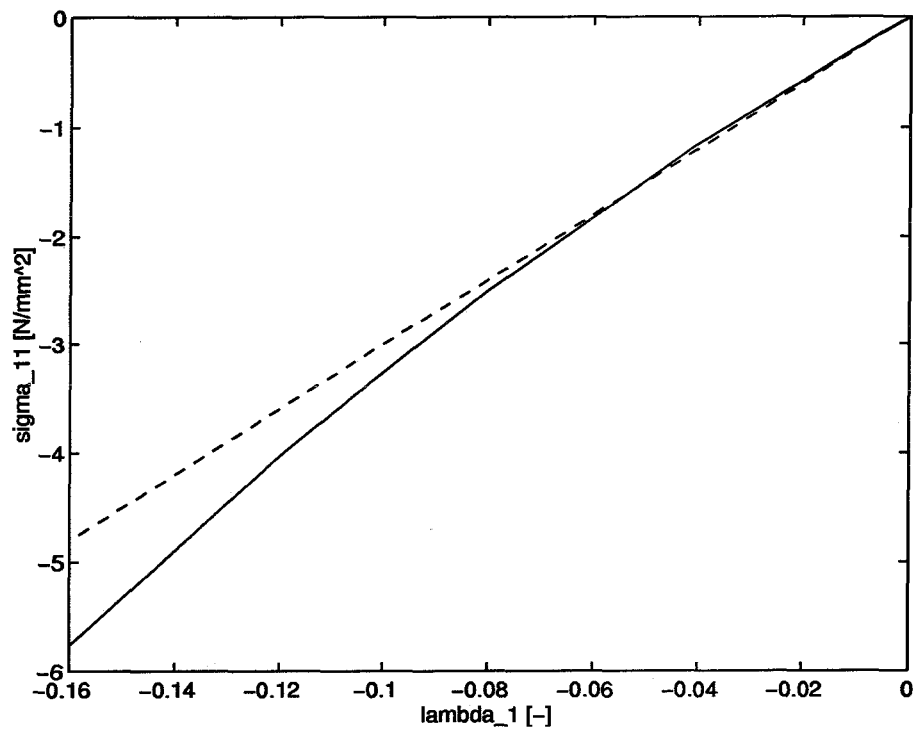τ_i = the Prony series relaxation time

Figure 3.6: The normalized stress-strain curve for a sample of one surface (curve) and its linear approximation (straight line).

variable	E_r N/mm^2	β_R sec	$\bar{g}_i^P$ for τ_i - sec
range of the value	0.4 - 40	0.002 - 0.02	0.5 10 0.2 60

Table 3.1: The range of the Young's modulus and Rayleigh damping ratio and the Prony series parameters for the surfaces.

The Prony series parameters are chosen for different relaxation times to approximate the material behavior. The shear modulus is related to the elastic modulus according to Equation 3.5 [2] for an isotropic material. Therefore, the time- dependence of the shear modulus has direct effects on the elasticity of the material. Since the stiffness of the running surface k_r is dependrnt on the elastic modulus of the rubber this introduces a time dependence of the stiffness of the surface.

$$E(t) = 2G(t)(1 + \nu) \tag{3.5}$$

where:
$E(t)$ = Young's modulus of elasticity as a function of time
$G(t)$ = the shear modulus as a function of time
ν = Poisson's ratio

Samples were taken from several multiple layer runing tracks. The layers of these samples were separated. The separate layers were submitted to compression tests up to $\lambda_1 = 0.5$ at a speed of 1 mm/min. They were also subjected to stress relaxation tests. From these tests, the range of the material properties was determined for the commercially available surfaces. The ranges can be found in Table 3.1. Only the Young's modulus has a range the other two are the same for all the tested surface materials.

variable	ρ kg/mm^3	ν -
value of the variable	$0.9 \cdot 10^{-6}$ - $1.2 \cdot 10^{-6}$	0.5

Table 3.2: The ranges of the density (ρ) and the Poisson's ratio as obtained from the literature.

variable	value	description
stepmax	3000	Max. number of steps in the analyses
ΔT_{max}	0.005	Max. interval size of one time step
ΔT_{min}	0.00000001	Min. interval size of one time step
T_{tot}	0.224	Total time of one stance phase
HAFTOL	50	Convergence criterium for one step

Table 3.3: The values of the ABAQUS variables as they were chosen for the calculations.

From the literature ([2], [3]) the values were chosen as shown in Table 3.2.

3.3 Computations

ABAQUS has to be provided with several parameters to perform dynamic nonlinear computations. The values for these parameters are determined for one typical surface and then used for all the surfaces. The values of the parameters are optimized for computational speed without loss of accuracy and were obtained through a series of test computations on the acrual surface. These values are found in Table 3.3.

Variable	Damping ratio (β_r)	Top layer Young's modulus (E_r)	Bottom layer Young's modulus (E_r)
used values	0.002	0.4	0.4
	0.005	1.0	0.4
	0.01	4.0	4.0
	0.02	10.0	10.0
		40.0	40.0

Table 3.4: The damping ratios and the stiffnesses of both layers as they were used for the calculations.

For the computations the density of the rubber was assumed to be $1.1 \cdot 10^{-6} kg/mm^3$ and constant across all materials. The Poisson's ratio had to equal 0.5 to represent incompressible material. The influence of Young's modulus of elasticity on the energy absorption of running surfaces was examined by choosing five moduli within the range of the tested surfaces. The elasticity of both the top and the bottom were varied independently which rendered 25 different surfaces. For these 25 surfaces the energies were calculated with four different damping ratios, thus 100 calculations were performed. The values for these three variables (the stiffness of the top layer, the stiffness of the bottom layer and the damping ratio) can be found in Table 3.4

The forces that were used for the input of the model were the same for each surface combination. These forces were force patterns for toe running as can be seen in Figure 3.7. The response of one of the surface combinations to this force pattern is displayed in Figure 3.8.
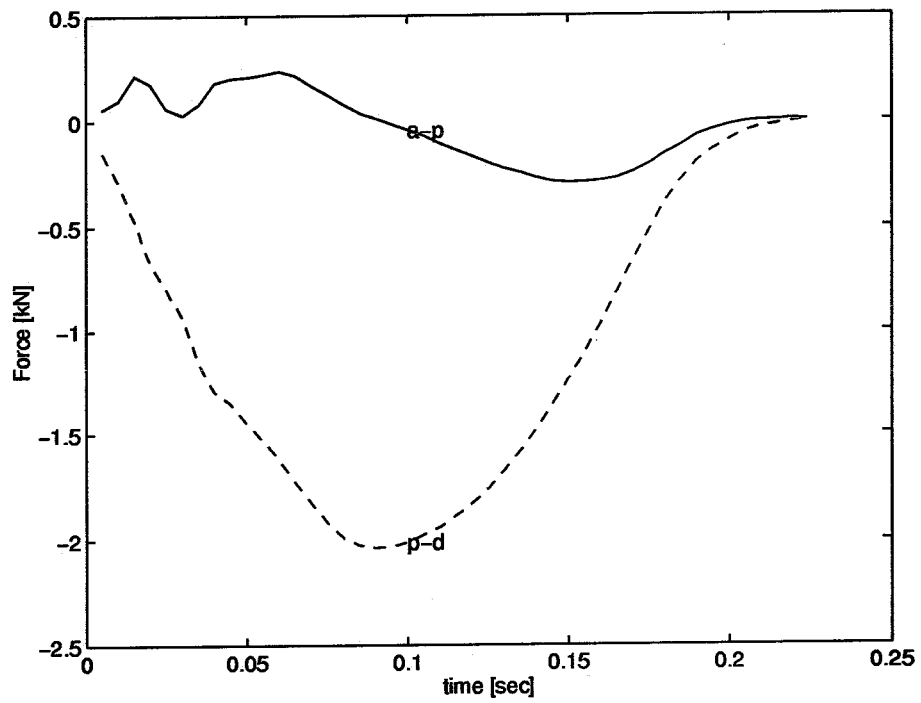
Figure 3.7: The forces as a function of time in both a-p and p-d direction that were applied to the contact area of every surface combination.
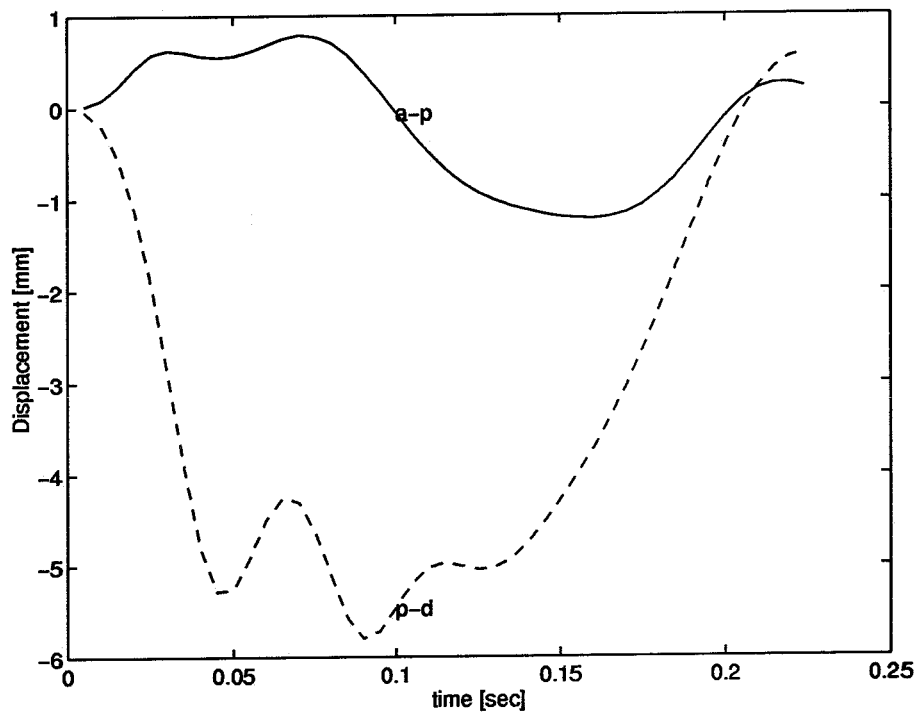
Figure 3.8: The calculated displacements as a function of the time for the contact area of a surface with top layer stiffness $= 10 \; N/mm^2$, bottom layer stiffness $= 0.4 \; N/mm^2$ and damping ratio $= 0.002 \; sec.$

Chapter 4

Results

The results of the calculations described in Chapter 3 are the displacements of all the nodes in the model. With the algorithms described in Chapter 2 the necesarry output variables were calculated. These are ERR, the Energy Return Ratio, U_{abs}, the absorbed energy, and U_{ret}, the returned energy values. The output variables consisted of values in both a-p and p-d directions. An example of the increase in absorbed and returned energy against the time in the a-p direction during one stance phase is illustrated in Figure 4.1. The values of the output depends on three variables: the damping of the surface, the stiffness of the top layer and the stiffness of the bottom layer of the surface. Each of the output variables will be discussed in more detail.

4.1 The Energy Return Ratio, ERR

The ERR was considerably greater in the p-d than in the a-p direction. The ERR_{a-p} was about 25% of the ERR_{p-d} (Figure 4.2). Since the ERR_{p-d} was greater it will be discussed first.

The energy return ratio in proximal-distal direction, ERR_{p-d}, was not substantially influenced by the stiffness of the top layer of the surface (Figure 4.3). The ERR_{p-d} was only influenced by the stiffness of the top layer if the bottom layer was very soft. Then increasing the stiffness of the top layer from very soft to very hard increased the ERR_{p-d} by 0.06. Also, if the damping of the surface increased, the ERR_{p-d} became influenced by the top layer stiffness (Figure 4.2). For a surface with low damping there was an increase in ERR_{p-d} of 0.03 as the top layer stiffness increased from 0.4 to 40.0 N/mm^2 and this increase became 0.08 for surfaces with high damping.
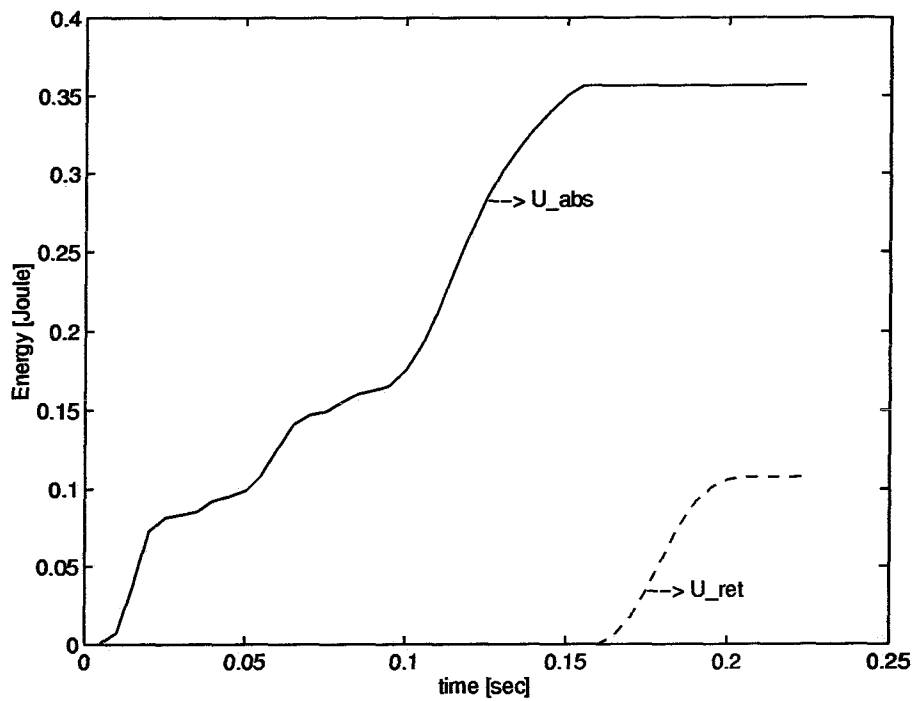
Figure 4.1: The absorbed energy in a-p direction, U_{abs}^{a-p} and the returned energy in a-p direction, U_{ret}^{a-p} against the time a surface with top layer stiffness = 10.0 N/mm^2, bottom layer stiffness = 0.4 N/mm^2, and damping ratio = 0.002 sec.
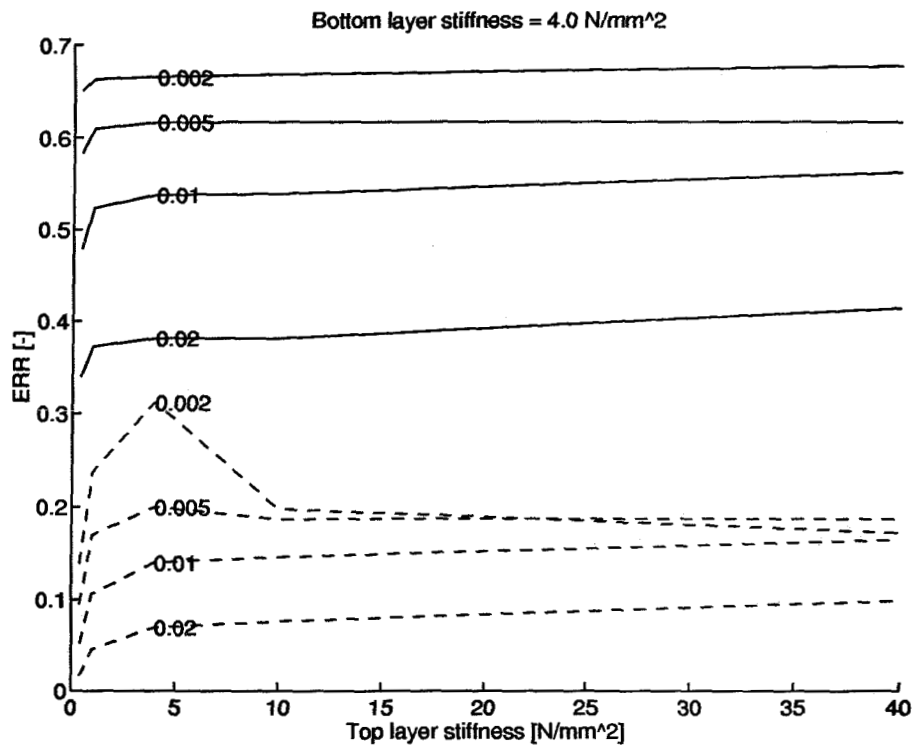
Bottom layer stiffness = 4.0 N/mm^2

Figure 4.2: The ERR_{p-d} (solid lines) and the ERR_{a-p} (dotted lines) as a function of the stiffness of the top layer for different damping ratios with a bottom layer stiffness of 4.0 N/mm^2.
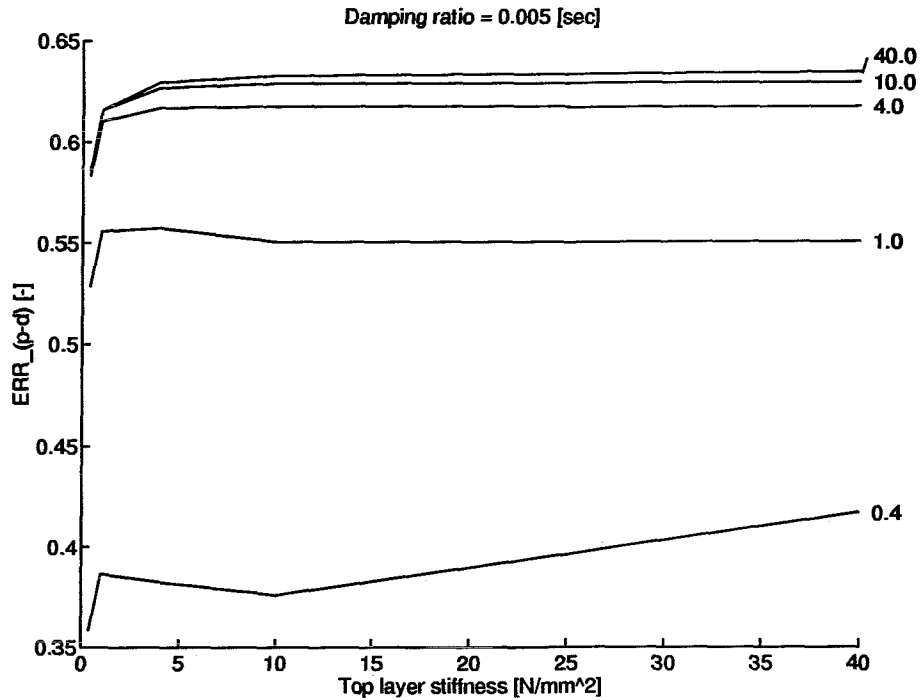
Figure 4.3: The ERR_{p-d} as a function of the stiffness of the top layer for different bottom layer stiffnesses and a damping ratio of 0.005 *sec*.

The ERR_{p-d} was influenced by the bottom layer stiffness. Increases in the bottom layer stiffness from 0.4 to 40.0 N/mm^2 increased the ERR_{p-d} by about 0.35 (Figure 4.4). However, the dominant increase occurred for changes of the bottom layer from 0.4 to 4.0 N/mm^2. As the damping of the surface increased, the ERR_{p-d} was influenced less by the bottom layer stiffness (Figure 4.2). For a surface with low damping there was an increase in ERR_{p-d} of 0.35 as the bottom layer stiffness increased from 0.4 to 40.0 N/mm^2 and this increase became 0.05 for surfaces with high damping (Figure 4.5).

The ERR_{p-d} was influenced by the damping ratio. Increases in the damping ratio from 0.002 to 0.02 *sec* decreased the ERR_{p-d} by 0.25 (Figure 4.3).
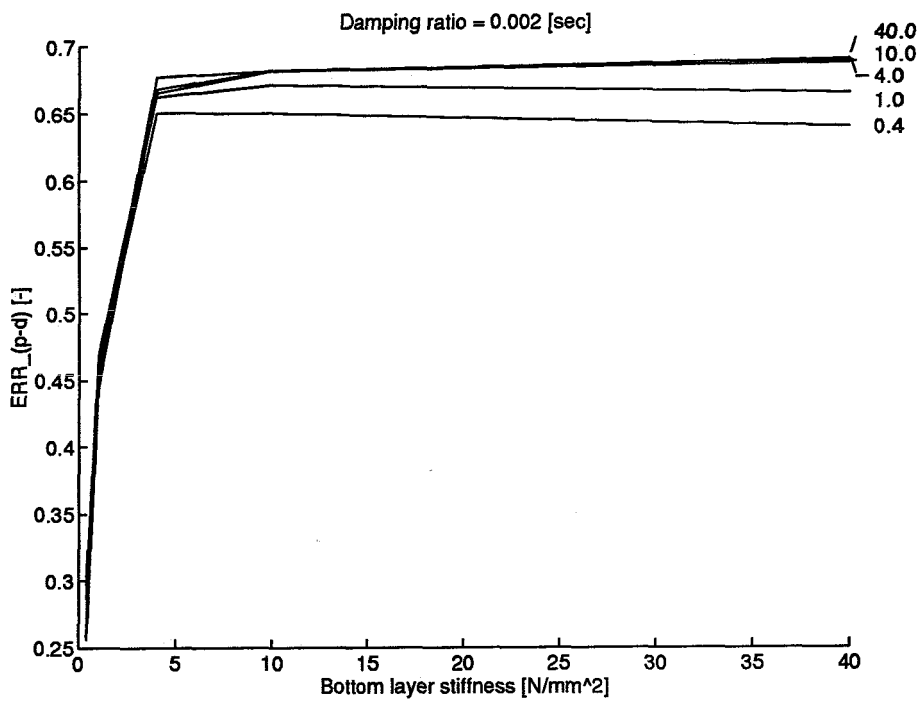
Figure 4.4: The ERR_{p-d} as a function of the stiffness of the bottom layer for different top layer stiffnesses and a damping ratio of 0.002 *sec*.
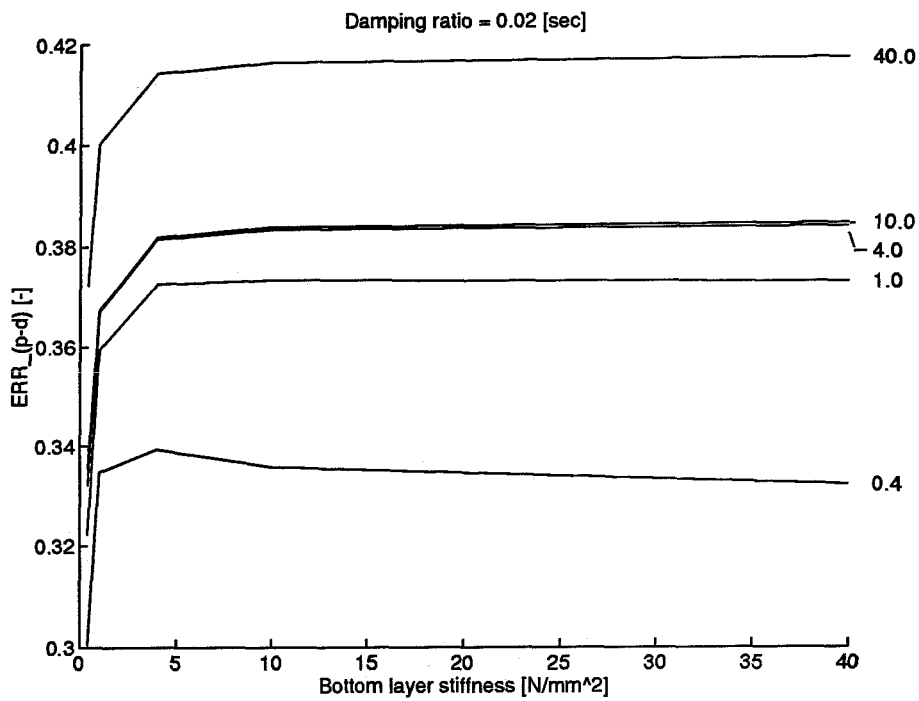
Figure 4.5: The ERR_{p-d} as a function of the stiffness of the bottom layer for different top layer stiffnesses and a damping ratio of 0.005 *sec.*
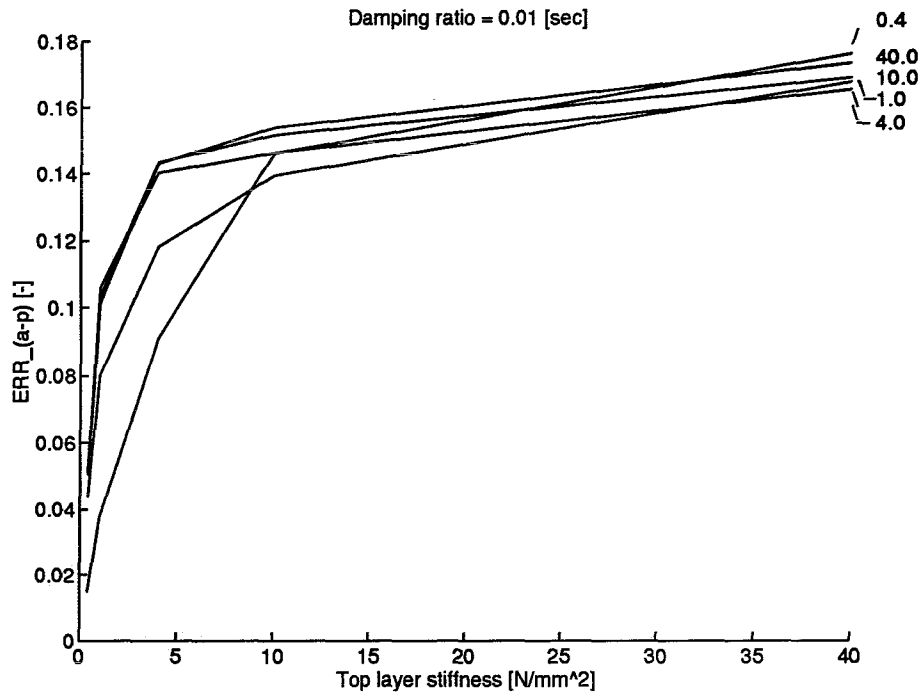
Figure 4.6: The ERR_{a-p} as a function of the stiffness of the top layer for different bottom layer stiffnesses and a damping ratio of 0.01 *sec*.

The energy return ratio in anterior-posterior direction, ERR_{a-p}, is predominantly influenced by the stiffness of the top layer of the surface (Figure 4.6). Increases of the top layer stiffness from 0.4 to 40 N/mm^2 increased the ERR_{a-p} by 0.12. The ERR_{a-p} as a function of the top layer stiffness had a maximum for a medium top layer stiffness and a very soft bottom layer (Figure 4.7). This maximum was 0.10 higher then the highest values for ERR_{a-p} with a medium to hard bottom layer. When the bottom layer stiffness was high, the influence of the top layer stiffness on the ERR_{a-p} became less. Also, if the damping of the surface increased, the ERR_{a-p} became less prone to display a maximum for certain combinations of top and bottom layer stiffnesses.

The bottom layer had no substantial effect on the ERR_{a-p} except for very soft bottom layers. For very soft bottom layers the ERR_{a-p} was up to 0.10 higher than for medium to hard bottom layers.
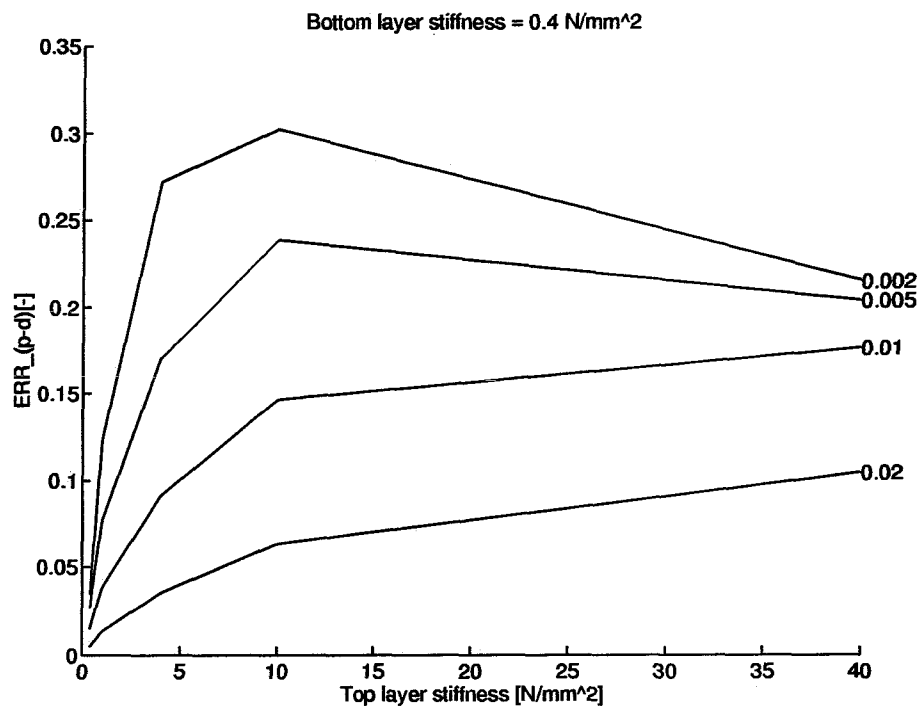
Results

33

Figure 4.7: The ERR_{a-p} as a function of the stiffness of the top layer for different damping ratios and a bottom layer stiffness of $0.4\ N/mm^2$.

Figure 4.8: The $U_{abs}{}^{p-d}$ as a function of the stiffness of the top layer for different bottom layer stiffnesses and a damping ratio of 0.002 *sec*.

The ERR_{a-p} was influenced by the damping ratio. For the stiffest top layer, increases in the damping ratio from 0.002 to 0.02 *sec* decreased the ERR_{a-p} by 0.15. In cases where the ERR_{a-p} displayed a maximum as a function of the top layer stiffness, i. e. for a top layers stiffness of $10 N/mm^2$ the ERR_{a-p} even decreased by 0.25 for increasing damping ratios.

4.2 The Absorbed Energy, U_{abs}

The absorbed energy in proximal-distal direction, $U_{abs}{}^{p-d}$, was substantially influenced by the stiffness of the top layer of the surface (Figure 4.8). Increasing the stiffness of the top layer from very soft $(0.4\ N/mm^2)$ to very hard $(40.0\ N/mm^2)$ decreased the $U_{abs}{}^{p-d}$ by about 4 Joules.
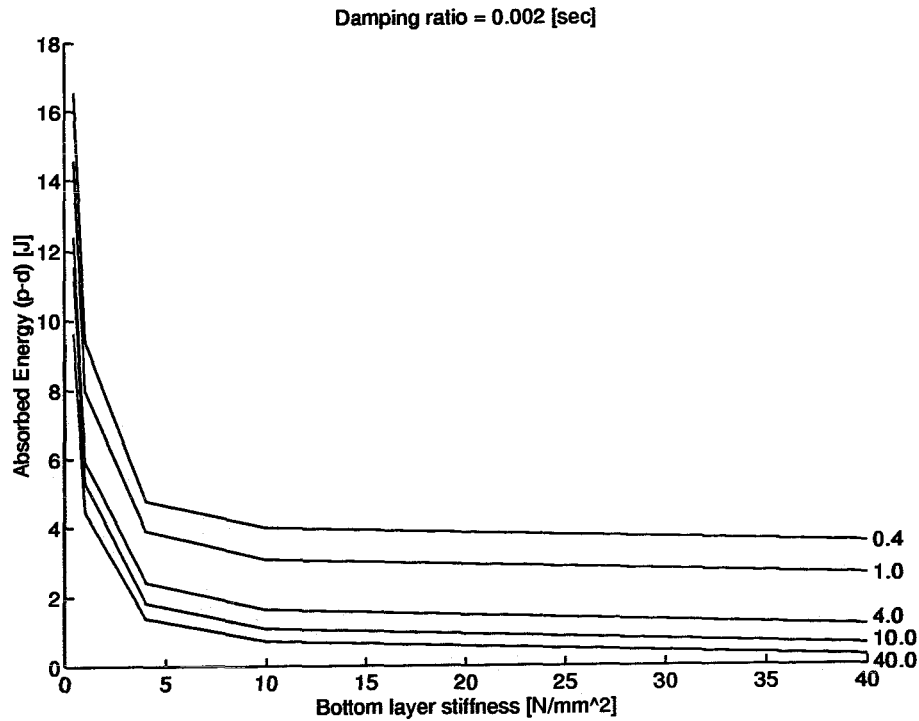
Damping ratio = 0.002 [sec]
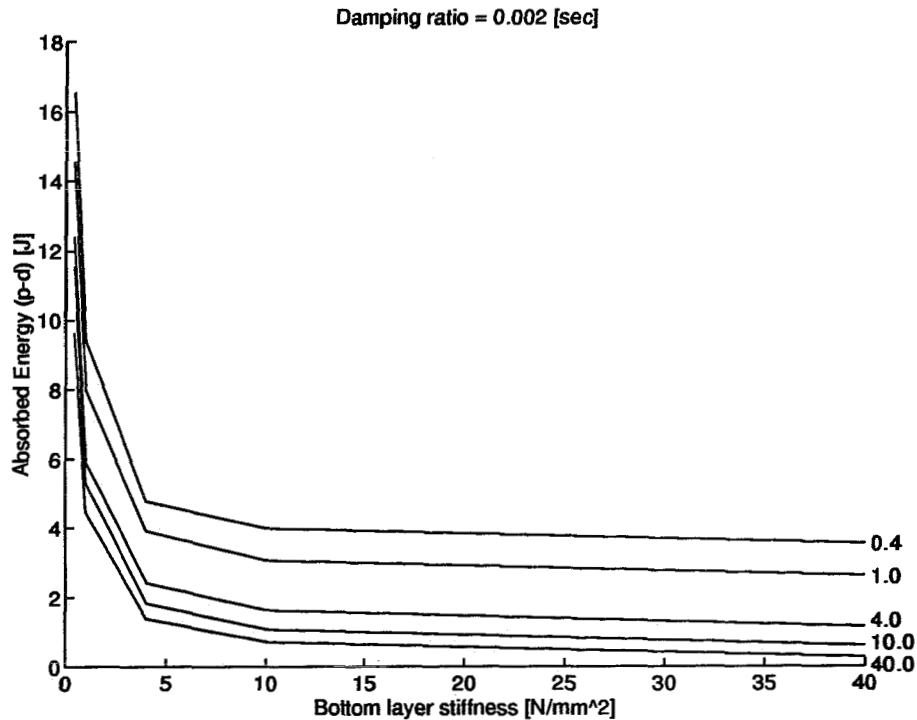
Figure 4.9: The $U_{abs}{}^{p-d}$ as a function of the stiffness of the bottom layer for different top layer stiffnesses and a damping ratio of 0.002 *sec*.

The $U_{abs}{}^{p-d}$, was dominantly influenced by the stiffness of the bottom layer of the surface (Figure 4.9). Increasing the stiffness of the bottom layer from very soft (0.4 N/mm^2) to very hard (40.0 N/mm^2) decreased the $U_{abs}{}^{p-d}$ by around 10 Joules. Therefore, the influence of the bottom layer stiffness on the $U_{abs}{}^{p-d}$ was considerably larger than the top layer stiffness.

Furthermore, the $U_{abs}{}^{p-d}$ was independent of the damping ratio of the surface unless the bottom layer stiffness was less than 1.0 N/mm^2. Then the $U_{abs}{}^{p-d}$ decreased with up to 4 Joules as the damping ratio's increased from 0.002 to 0.02 *sec*.

The absorbed energy in anterior-posterior direction, $U_{abs}{}^{a-p}$, was strongly influenced by the stiffness of the top layer of the surface. Increasing the stiffness of the top layer from very soft (0.4 N/mm^2) to very hard (40.0 N/mm^2) decreased the $U_{abs}{}^{a-p}$ by 1.5 Joules. If the bottom layer became very soft the $U_{abs}{}^{a-p}$ decreased by 4 Joules for increasing top layer stiffnesses.

The $U_{abs}{}^{a-p}$ was independent of the bottom layer stiffness unless the stiffness of the top layer was less than 1.0 N/mm^2. In that case the $U_{abs}{}^{a-p}$ decreased by up to 2 Joules as the stiffness of the bottom layer increased. The greatest decrease in $U_{abs}{}^{a-p}$ occurred for bottom layer stiffnesses between 0.4 and 4.0 N/mm^2.

Furthermore, the $U_{abs}{}^{a-p}$ was independent of the damping ratio of the surface.

4.3 The Returned Energy, U_{ret}

The returned energy in proximal-distal direction, $U_{ret}{}^{p-d}$, was substantially influenced by the stiffness of the top layer of the surface. Increasing the stiffness of the top layer from very soft (0.4 N/mm^2) to very hard (40.0 N/mm^2) decreased the $U_{ret}{}^{p-d}$ by up to 2 Joules for surfaces with low damping ratios. However as the damping ratios increased, the decrease in $U_{ret}{}^{p-d}$ for the range of top layer stiffnesses dropped to 1 Joule.

The $U_{ret}{}^{p-d}$ was predominantly influenced by the stiffness of the bottom layer of the surface. Increasing the stiffness of the bottom layer from 0.4 N/mm^2 to 40.0 N/mm^2 decreased the $U_{abs}{}^{p-d}$ by 2 Joules for surfaces with low damping ratios. However, for surfaces with high damping ratios the $U_{abs}{}^{p-d}$ decreased by 1.5 Joules.

The damping ratio influenced the $U_{ret}{}^{p-d}$ considerably. For soft top and bottom layers the $U_{ret}{}^{p-d}$ decreased by 1 Joule for an increase in the damping ratio between 0.002 and 0.02 *sec*. For hard top and bottom layers this decrease was 0.4 Joules.

The returned energy in anterior-posterior direction, $U_{ret}{}^{a-p}$, was substantially influenced by the stiffness of the top layer of the surface. Increasing the stiffness of the top layer from very soft (0.4 N/mm^2) to very hard (40.0 N/mm^2) decreased the $U_{abs}{}^{p-d}$ by up to 0.5 Joules for surfaces with low damping ratios. However as the damping ratios increased the decrease in $U_{abs}{}^{p-d}$ for the range of top layer stiffnesses dropped to 0.2 Joule.

The $U_{ret}{}^{p-d}$ was not influenced by the stiffness of the bottom layer of the. Only for very soft bottom layers there was a decrease of 0.1 Joule in the $U_{ret}{}^{p-d}$.

The damping ratio influenced the $U_{ret}{}^{a-p}$ considerably for soft top and bottom layers. For soft top and bottom layers the $U_{ret}{}^{a-p}$ decreased by 0.2 Joule for an increase in the damping ratio between 0.002 and 0.02 *sec*. The influence of the damping ratio was negligible for hard top and bottom layers.

Chapter 5

Discussion

5.1 Model

The algorithms used to calculate the energy that is absorbed and returned used two assumptions. First, they assumed that energy that is returned before a certain phase of the stride cannot be used to aid in take off. Secondly, they assumed that the energy that is returned before it can be used for take off is energy that the body has to absorb. Both these assumptions are reasonable since vibrations of the surface on impact are not used to facilitate take off, in fact they have to be absorbed in the leg which has to react to these vibrations. This time factor has, to the knowledge of the author, never been used to calculate energy return in running.

The FEM assumed that the forefoot is a rigid plate with even pressure distribution. It also assumed that the shape and size of this plate does not change and that the position of the plate does not change. These simplifications can ultimately only be justified by repeating the calculations with a flexible forefoot and a realistic pressure distribution under the forefoot. However, it is not expected that these alterations will influence the results considerably since toe running is usually done in spike-shoes which have a relatively hard plate under the forefoot.

Most studies on energy in running assumed that the only direction of interest is the vertical direction ([10], [14]). In this study the anterior-posterior direction was modelled and even though the energies were 25 % of the p-d direction, there was a considerable amount of energy dissipated in the a-p direction (up to 5 Joules). In the future, this direction should not be neglected.

The rubber of the running surface was modelled as a linear spring with a linear damper. Since the deformations were relatively small this assumption seems acceptable. The main difference with other studies([10], [14]) is that the present study used continuum finite elements to describe the surface. Other studies approximated the surface with either one or with several discrete spring-damper systems. The disadvantage with spring-damper systems is that there can be no a-p displacement or force. Also the shear modulus and the incompressibility of the material is typically not accounted for, rendering elevated stress gradients and decreased material stiffness around areas with high stress gradients.

5.2 Energy Return Ratio, Absorbed and Returned Energy

The results can be divided in results for the anterior-posterior direction and results for the distal-proximal direction. The results for both directions will be discussed seperately. The range of the results for the absorbed energy coincides with the values that are found in the literature ([12], [14]). The results ranged from 15 Joules energy absorbed during one stride for very soft surfaces to less than 1 Joule for very hard surfaces.

The energies that were absorbed and returned were about four times larger in the p-d direction than in the a-p direction. This is due to the fact that both the displacements and the exerted forces are considerably smaller in a-p direction than in p-d direction.

5.2.1   p-d direction

For the p-d direction, the decrease of the ERR_{p-d} for softer material can be explained with the fact that as the stiffness decreases the deformation increases. The deformation speeds will be greater as a result of the increased deformations. As the deformation speed increases, so does the viscous part of Equation 2.10 and 2.11. This increase of the viscous component implies that U_{abs} in Equation 2.10 will increase and that U_{ret} in Equation 2.11 will decrease. Since ERR_{p-d} is defined by Equation 2.13 this means that with increasing deformation speed the ERR_{p-d} decreases. As the stiffness of the surface increases the deformation and thus the deformation speed decreases. Therefore the viscous effect of the surface becomes negligible so more energy can be recovered from the surface, explaining the increase in the ERR_{p-d} for increasing stiffness.

The absorbed energy is mainly dependent on the stiffness of both the top and the bottom layer. This can be explained as follows. For a linear spring the stored energy after compression with a given force is described by Equation 5.1.

$$U_{abs} = \frac{1}{2}kx^2 \tag{5.1}$$

where:
U_{abs} = the stored energy
k = the stiffness of the surface (which is a function of E)
x = the displacement

Since x is given by Equation 5.2,

$$x = F/k \tag{5.2}$$

The energy that is stored can be written as shown in Equation 5.3.

$$U_{abs} = \frac{1}{2}F^2/k \tag{5.3}$$

From Equation 5.3 , it can be seen that if E increases the absorbed energy decreases. This explains the hyperbolic shape of Figures 4.8 and 4.9 since the surface behaves like a linear spring to a certain extent. The reason why the damping has hardly any influence on the absorbed energy is that with increased damping the viscous component of the absorbed energy increases while at the same time the elastic component of the absorbed energy decreases. The elastic component of the absorbed energy decreases because the displacements are reduced since the material is relatively stiffer.

The returned energy depends on the absorbed energy since energy that was not absorbed cannot be returned. This is supported by the fact that the returned energy depends on the stiffness of the top and bottom layers of the surface. However, contrary to the absorbed energy, the damping ratio does influence the returned energy which can be explained as follows: As the force decreases towards the toe-off the surface moves in proximal direction. The distance travelled depends on the speed at which the surface travels so the distance travelled is directly correlated to the damping ratio. A high damping ratio implies less distance travelled so less returned energy. Or, in other words, the viscous term in Equation 2.11 is larger so the returned energy is smaller for higher damping ratios.

5.2.2   a-p direction

In general the same principles used to explain the behavior of the surface
in p-d direction can be applied to the a-p direction. However, since dis-
placements in the a-p direction mainly depend on shear, the top layer will
have a great influence on the performance of the surface. This because the
displacements in both directions are the greatest in the top layer. For the
a-p direction the following occurs. At the edges of the contact area this
area pushes against the non-loaded surface. Since the displacements are
the greatest in the top layer, the stiffness of the non-loaded surface in the
top layer has a great influence on the actual displacements that occur. The
effect is greater in the a-p direction than in the p-d direction since in the
a-p direction the interface between the non-loaded and the loaded surface is
loaded with a compression type loading so the Young's modulus applies to
calculate the displacements that occur. In the p-d direction, the interface
between the non-loaded and the loaded part of the surface is loaded with a
shear type loading so the shear modulus applies for the displacements that
occur. This shear modulus is a factor 3 smaller than the Young's modulus
as can be seen from Equation 3.5.

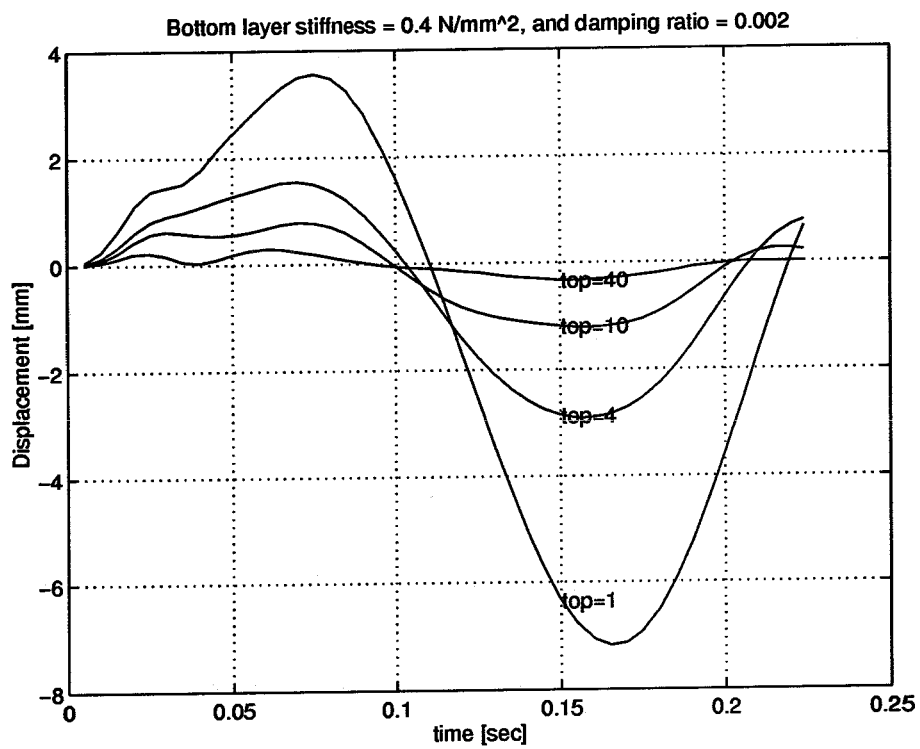**Bottom layer stiffness = 0.4 N/mm^2, and damping ratio = 0.002**

Figure 5.1: The displacement in the a-p direction of the contact area of a surface as a function of time for different top layer stiffnesses for a bottom layer stiffness of 0.4 N/mm^2 and a damping ratio of 0.002 sec.

The peak that is found in the ERR_{a-p} for soft bottom layers is due to the fact that for soft bottom layers the surface is well tuned. In **Figure 5.1** one can see that the displacements in the a-p direction for a surface with a bottom stiffness of 0.4 N/mm^2 and a damping ratio of 0.002 are not zero at the moment of toe-off. They are positive, meaning that the surface has pushed the foot forward. This explains an increase in returned energy. The ERR_{a-p} has a maximum for top stiffness of 10.0 N/mm^2 because at the toe-off the surface is almost at the maximum extension and has no kinetic energy stored in it (as indicated by the nearly horizontal shape in Figure 5.1) whereas the surfaces with other top layer stiffness are not as close to maximum extension at toe-off as their slopes are not horizontal.

5.3   Future Research

For the a-p direction an optimal combination of top layer stiffness, bottom layer stiffness, and damping ratio was found ($10N/mm^2, 0.4N/mm^2$ and $0.002sec$ respectively). This combination rendered a ERR_{a-p} that was considerably higher than for combinations that were not optimal. Of course an optimal combination exists for the p-d direction. Future research could focus on finding this combination of top layer stiffness, bottom layer stiffness and damping ratio.

There is, however, a conflict of interest between the a-p and the p-d direction. The ERR_{a-p} benefits from a soft bottom layer and a hard top layer (10 N/mm^2) whereas the ERR_{p-d} benefits from a hard bottom layer. Research in running surfaces could also focus on finding a running surface that is stiff in p-d direction and soft in a-p. Also the tuning of the surface as seen in Figure 5.1 can also be achieved in p-d direction. This is a matter of finding the right parameters. This is also an area of interest but since the ERR_{p-d} is already relatively high, the expected gain will be small.

This project focuses on the energy aspects of running from a surface point of view. This does not imply that the solutions found in this report are the optimal solutions for the human body. For instance, high damping of a surface causes a reduced ERR. This would imply that surfaces with high damping would not be favourable. There is a possibility that damping has a possitive effect on the human body in that it decreases the vibrations of the surface that otherwise would have to be absorbed by the body. Future research could include the human body in the model presented in this project to investigate if this would alter the optimal solutions.

Chapter 6

Summary – Conclusion

Several conclusions can be drawn from this project.

First of all, the method used here gives feasible results. The values of the absorbed energies have the same order of magnitude as those found in the literature. Also, the curves that result from varying the bottom layer stiffness, the top layer stiffness and the damping ratio are as expected.

Second, from the surface point of view damping is not a wanted comodity in running surfaces since it influences the amount of energy that is returned. In all the results an increasing damping ratio caused for less returned energy and for a smaller ERR.

Third, the absorbed or the returned energy does not diminish considerably if the surface is stiffer than 10.0 N/mm^2. Therefore, it is questionable to use very hard surfaces since the benefits are relatively small. Maybe the benefits of using very hard surfaces do not outweigh the costs of increased injuries.

Also, this project has shown the need to include the a-p direction in the analyses of running surfaces. Eventhough the dissipated energies in this direction are less than those in the p-d direction, they are not negligible. It is however not clear which of the two directions is the most important. To assess the priority of both directions the human body needs to be included in the model.

Finally, there is a conflict of interest between the a-p and the p-d direction. The ERR_{a-p} benefits from a soft bottom layer and a hard top layer (10 N/mm^2) whereas the ERR_{p-d} benefits from a hard bottom layer. No combination of surface properties has been found that optimizes the surface in both directions.

Bibliography

[1] J. J. Aklonis and W. J. MacKnight. *Introduction to Polymer Viscoelasticity*. John Wiley and Sons, 1983.

[2] R. G. C. Arridge. *Mechanics of Polymers*. Clarendon Press, 1975.

[3] C. M. Blow and C. Hepburn, editors. *Rubber Technology and Manufacture*. Butterworth Scientific, 1982.

[4] M. F. Bobbert, H. C. Schamhardt, and B. M. Nigg. Calculation of vertical ground reaction force estimates during running from positional data. *Journal of Biomechanics*, 24:1095–1105, 1991.

[5] E. C. Frederick, T. E. Clarke, J. L. Larsen, and L. B. Cooper. The effects of shoes and surfaces on the economy of locomotion. In B. M. Nigg and B. A. Kerr, editors, *Biomechanical Aspects of Sport Shoes and Playing Surfaces*, pages 107–114. University Printing,Calgary, 1983.

[6] H. Hess and W. Hort. Erhoehte verletzungsgefahr beim leichtathletiktraining auf kunststoffboden (increased danger of injuries during practicing track and field on artificial surfaces). *Sportartzt Sportmed.*, 12:282–285, 1973.

[7] R.S. Marvin. The linear viscoelastic behavior of rubberlike polymers and its molecular interpretation. In J. T. Bergen, editor, *Viscoelasticity*, pages 27–54. Academic Press, 1960.

[8] P. J. J. McCullagh and I. D. Graham. A preliminary investigation into the nature of shock absorbency in synthetic sports materials. *Journal of Sports Sciences*, 3:103–114, 1985.

45

[9] T. A. McMahon and P. R. Greene. The influence of track compliance on running. *Journal of Biomechanics*, 12:893–904, 1979.

[10] B. M. Nigg and W. Herzog, editors. *Biomechanics of the musculo-skeletal system*, chapter 4.4, pages 424–433. John Wiley and Sons, 1994.

[11] B. M. Nigg and B. Segesser. The influence of playing surfaces on the load on the locomotor sustem and on football and tennis injuries. *Sports Medicine*, 5:375–385, 1988.

[12] B. M. Nigg and B. Segesser. Biomechanical and orthopedic concepts in sport shoe construction. *Medicine and Science in Sports and Exercise*, 24(5):595–602, 1992.

[13] B. M. Nigg and M. R. Yeadon. Biomechanical aspects of playing surfaces. *Journal of Sports Sciences*, 5:117–145, 1987.

[14] M. R. Shorten. The energetics of running and running shoes. *Journal of Biomechanics*, 26:41–51, 1993.

[15] G. Tipp and V. J. Watson. *Polymeric Surfaces for Sports and Recreation*. Applied Science Publishers, 1982. ISBN 0-85334-980-0.

[16] various. *Abaqus User's Manual I*. Hibbitt, Karlson and Sorensen, 1993.

[17] M. R. Yeadon and B. M. Nigg. A method for the assessment of area-elastic surfaces. *Medicine and Science in Sports and Exercise*, 20(4):403–407, 1988.